Thermodynamic Properties of the Geothermal Resources (Khachmaz and Sabir-Oba) of Azerbaijan

N. D. Nabiyev,[†] M. M. Bashirov,[†] J. T. Safarov,*[,†,‡] A. N. Shahverdiyev,[†] and E. P. Hassel[‡]

Azerbaijan Technical University, H. Javid Avenue 25, AZ1073 Baku, Azerbaijan, and Lehrstuhl für Technische Thermodynamik, Universität Rostock, 18059 Rostock, Germany

The (p, ρ, T) properties of two geothermal resources of Azerbaijan at T = (278.15 to 373.15) K and pressures up to p = 40 MPa are reported. An empirical correlation for the density of the geothermal resources as a function of pressure and temperature has been developed. The equation was used to calculate other volumetric properties such as isothermal compressibility, isobaric thermal expansibility, and difference in isobaric and isochoric heat capacities.

Introduction

Geothermal energy harnesses the heat energy present underneath the Earth and is generated in many places, where heat from the earth's core rises to the surface, for example, where volcanoes and hot springs are present. This heat can also be exploited by drilling down (3 to 5) km to reach "hot rocks" with temperatures at or above 200 °C.

People have used the geothermal energy resources for bathing, cooking, and heating. Hot water near the earth's surface can be piped directly into buildings and industries for heat. A district heating system provides heat for 95 % of the buildings in Reykjavik, Iceland. Examples of other direct uses include growing crops and drying lumber, fruits, and vegetables.

Azerbaijan possesses rich geothermal energy and mineral water resources, which can be divided into the following regions (Figure 1):[1] Nakhichivan, Greater Caucasus- Pre-Caspian, Lesser Caucasus, Talish mountains, Samur-Devechi piedmont, Absheron peninsula, and Kura-Araz depression.[2,3] More than 50 million cubic meters of geothermal energy resources are available in Azerbaijan with maximum temperatures of up to ~ 140 °C. The exploitation of the geothermal energy and mineral resources has proved to be economically viable, and many industrial plants producing iodine, bromine, boron, arsenic, liquid carbon dioxide, various salts, and other products have been constructed. The heat content of the water, which is equivalent to that obtained by burning about 20 000 tonnes of coal, could also be used in various spheres of the national economy. The potential of these geothermal resources is therefore huge because they contain an inexhaustible amount of heat energy that could be successfully used for heating sanatorium-resort complexes, populated areas, medical and communal buildings, and sports venues and for the supply of hot water and electricity.[1]

The geothermal energy and mineral water resources of Azerbaijan can potentially be used for bottled water production and medicinal purposes and for spas and health clinics that utilize the water to treat arthritis, dysfunction of the nervous system, and skin diseases. But they can also be used for thermal heating and for warming soil, hotbeds, and hothouses with the aim of early and rapid growth of vegetables and fruits at (40 to 50) °C. This could provide three harvests per season. Taking tomatoes and cucumbers as an example, on the basis of current prices for these products, the return period for an investment in a covered greenhouse using thermal water would be (1.5 to 2) years. Geothermal resources with higher temperature ((80 to 100) °C and higher) can be used for the generation of electricity.

The geothermal resources of Azerbaijan have been extensively studied,[4−7] but most of these research investigations were of geological, geographical, and chemical properties. The main thermophysical properties, such as density, viscosity, vapor pressure, and so on have had only limited studies. Using the geothermal energy resources of Azerbaijan as an alternative energy source requires the investigation of the thermophysical properties of a wide range of parameters. In many cases, the temperature of the geothermal water remains high, but pressure quickly becomes equal to ambient pressure. If we use the geothermal resources for power generation directly at the source, then they can be generating the energy. Using experience in Iceland and other developed countries, we can maximize the use of geothermal energy as an alternative energy resource.

Azerbaijan's part of the Greater Caucasus region and Pre-Caspian ((800 to 3385) m) region are rich in geothermal energy resources. The temperature of the water fluctuates around 90 °C, and the estimated discharge is about 4.0 million liters per day. The waters are dominated by sodium bicarbonate composition. H_2S waters are found on the south and southeast slope of the Greater Caucasus and are confined to sedimentary deposits. Fresh hot calcium−sodium-bicarbonate waters were found with temperatures of up to 90 °C. Some geothermal resources have a depth of 1400 m. The waters are imbibed. The main conditions treated are diseases of the stomach, the liver and biliary ducts, the kidneys, and the urethra canal, urology, and metabolic disorders. The main chemical components are: Cu, Br, I, F, Mn, Ti, H_2S, Sr, and so on.[1−3]

The main objective of this article is to provide accurate experimental density data of the geothermal resources of the second geothermal region of Azerbaijan (Greater Caucasus- Pre-Caspian) at T = (278.15 to 373.15) K and at pressures up to p = 40 MPa using a vibrating tube densimeter. For this purpose, the (p, ρ, T) properties of the Khachmaz and Sabir-Oba

* To whom correspondence should be addressed. Tel: +49 381 4989415. Fax: +49 381 4989402. E-mail: javid.safarov@uni-rostock.de.
[†] Azerbaijan Technical University.
[‡] Universität Rostock.

10.1021/je800840m CCC: $40.75
Published on Web 04/14/2009

Figure 1. Geothermal energy and mineral water resources of Azerbaijan.

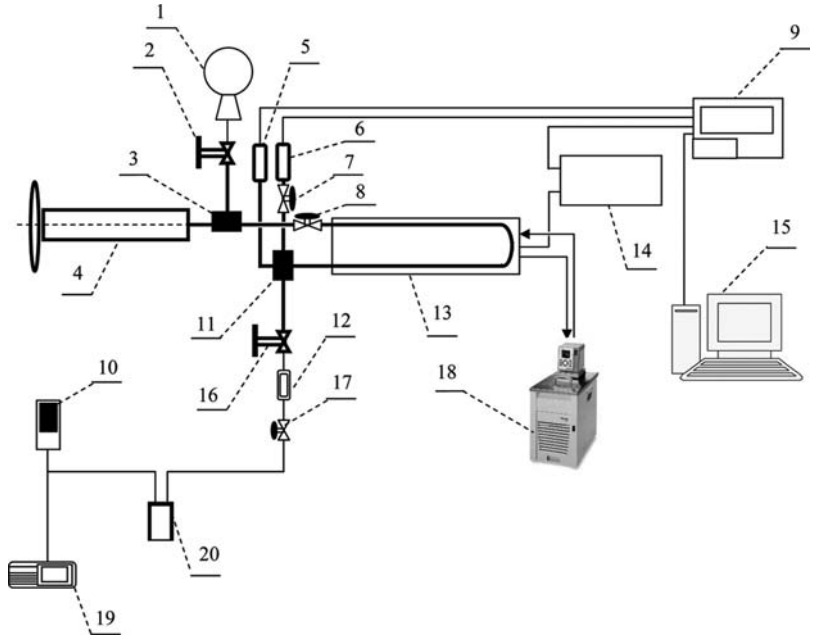

Figure 2. New modernized high-pressure−high-temperature vibrating tube densimeter DMA HPM: 1, flask for the probe; 2, 7, 16, 17, valves; 3, 11, fitting; 4, pressure manometer; 5, pressure sensor HP-1; 6, pressure sensor P-10; 8, valve for the closing of system during the experiments; 9, display mPDS2000V3 for the temperature and frequency control; 10, vacuum indicator; 12, visual window; 13, vibration tube; 14, interface mode; 15, PC; 18, thermostat F32-ME; 19, vacuum pump; 20, thermos for cooling.

geothermal resources of the Khachmaz region of Azerbaijan have been examined for the first time.

Thermodynamic properties of these geothermal resources are not available in the literature, and a comparison of them with those from literature was impossible. The experimental results were described using an equation of state.

Experimental Section

The chemical compounds of samples were analyzed in the IRIS Intrepid II optical emission spectrometer (OES). The IRIS Intrepid II OES series is a family of inductively coupled argon plasma (ICP) OESs that use Echelle optics and a unique charge injection device (CID) solid-state detector to provide superb

Table 1. Chemical Analysis of the Measured Geothermal Resources

minerals in the samples in mg·L^{-1}	Khachmaz	Sabir-Oba
Al	<0.01	<0.01
As	0.01	0.01
B	4.30	1.40
Ba	0.04	0.23
Ca	89.1	78.2
Cd	<0.01	<0.01
Co	<0.01	<0.01
Cr	<0.01	<0.01
Cu	<0.01	<0.01
Fe	0.03	0.11
Hg	<0.02	<0.02
K	9.50	9.50
Fe	0.03	0.11
Li	0.19	0.13
Mg	13.60	9.46
Mn	0.06	0.06
Mo	0.05	0.02
Na	882	736
Ni	<0.01	<0.01
P	<0.01	<0.01
Pb	<0.01	<0.01
S	220	24.60
Sb	<0.02	<0.02
Se	<0.02	<0.02
Si	6.19	4.36
Sr	3.92	5.12
Ti	0.13	<0.01
Tl	0.12	<0.05
V	<0.01	<0.01
Zn	<0.01	<0.01

sensitivity and selectivity. These systems provide complete and continuous wavelength coverage over the analytical wavelength range from (165 to 1000) nm. When the optional XUV configuration is employed, the range is extended to 130 nm. Concentrations in the low ppb to the percent range can be readily determined. All operations of the spectrometer are controlled by the TEVA (thermo electron validated analysis) software, which runs under Microsoft Windows XP Professional.

The (p, ρ, T) measurements were carried out using a new modernized high-pressure−high-temperature vibrating tube densimeter DMA HPM (Anton-Paar, Austria). The schematic principle of the vibration tube densimeter is shown in Figure 2. The measurements with a vibrating tube (13) are based on the dependence between the period of oscillation of a unilaterally fixed U-tube Hastelloy C-276 and its mass. This mass consists of the U-tube material and the mass of the fluid filling the U-tube. The behavior of the vibrating tube can be described by the simple mathematical−physical model of the undamped spring-mass system.[8] The characteristic period of oscillation τ (microseconds) of this model is described by the following equation

$$\tau(T,p) = 2\pi\sqrt{\frac{m_0 + \rho(T,p)V(T,p)}{k}} \qquad (1)$$

where $\tau(T, p)$ is the period of oscillation of the vibration tube in microseconds; m_0 is the mass of the empty vibrating tube in kilograms; $V(T, p)$ is the volume of the vibrating tube in cubic meters; $\rho(T, p)$ is the sample density in kilograms per cubic meter; and k is the spring constant in newtons per meter.

The period of oscillation measurement and the temperature control are implemented within the DMA HPM control system, which consists of a measuring cell (13) and a modified mPDS2000V3 control unit (9) connected to a PC (15) via an interface (14). The temperature in the measuring cell was controlled using a thermostat (18) F32-ME (Julabo, Germany) with an error of ±10 mK and was measured using the (ITS-90) Pt100 thermometer with an experimental error of ±15 mK. Pressure was created by a pressure intensifier (4) (HIP, type 37-6-30) and measured by a pressure transmitter (6) (P-10,

Table 2. Experimental Values of Pressure, p/MPa, Density, ρ/kg·m^{-3}, Temperature, T/K, Isothermal Compressibility, k_T·10^6/MPa^{-1}, Isobaric Thermal Expansibility, α_p·10^6/K^{-1}, and Difference in Isobaric and Isochoric Heat Capacities, ($c_p - c_v$)/J·kg^{-1}·K^{-1}, of the Khachmaz Geothermal Resource of Azerbaijan from T = (278.14 to 373.00) K

p	ρ	T	k_T·10^6	α_p·10^6	$c_p - c_v$
0.624	1004.04	278.15	499.1	102.6	5.8
5.004	1006.21	278.15	490.9	120.5	8.2
10.023	1008.65	278.16	481.9	140.5	11.3
15.012	1011.05	278.15	473.3	160.0	14.9
20.035	1013.43	278.14	465.1	179.2	18.9
25.036	1015.76	278.15	457.1	198.0	23.5
30.054	1018.07	278.15	449.5	216.6	28.5
35.124	1020.37	278.14	442.2	234.9	34.0
40.021	1022.56	278.15	435.3	252.5	39.8
0.539	1002.59	288.14	466.5	194.4	23.3
5.006	1004.66	288.16	458.8	205.4	26.4
9.855	1006.87	288.17	450.8	216.9	29.9
15.151	1009.25	288.17	442.5	229.0	33.8
20.064	1011.43	288.17	435.1	239.9	37.7
25.121	1013.64	288.16	427.8	250.7	41.8
30.103	1015.79	288.16	420.9	261.2	46.0
35.111	1017.92	288.16	414.1	271.5	50.4
40.145	1020.04	288.15	407.7	281.5	54.9
1.025	1000.15	298.27	447.9	271.7	49.1
5.079	1002.02	298.22	441.4	276.7	51.6
9.818	1004.22	298.22	433.8	282.9	54.8
15.593	1006.61	298.17	425.9	289.0	58.1
20.018	1008.46	298.13	420.0	293.6	60.7
25.104	1010.69	298.13	412.9	299.3	64.0
30.155	1012.85	298.12	406.2	304.5	67.2
35.089	1014.82	298.13	400.2	309.3	70.2
40.040	1016.88	298.13	394.1	314.0	73.3
0.898	995.52	313.08	436.8	376.5	102.1
4.995	997.25	313.10	431.2	377.3	103.7
9.972	999.20	313.15	425.1	378.2	105.5
15.563	1001.65	313.17	417.6	378.7	107.4
20.008	1003.42	313.20	412.3	379.0	108.7
25.534	1005.80	313.18	405.5	378.6	110.1
30.057	1007.65	313.19	400.2	378.3	111.1
35.586	1009.82	313.17	394.3	377.4	112.0
39.970	1011.52	313.15	389.7	376.6	112.6
1.160	989.32	328.02	438.5	481.4	175.3
5.024	990.99	328.04	433.8	479.9	175.7
10.079	993.00	328.17	428.3	478.4	176.5
15.576	995.38	328.18	422.1	475.2	176.4
19.985	997.22	328.19	417.4	472.5	176.0
25.527	999.61	328.17	411.5	468.4	175.0
30.023	1001.50	328.14	407.0	464.7	173.8
35.513	1003.58	328.12	402.2	460.4	172.3
39.978	1005.37	328.06	398.1	456.2	170.6
0.846	981.22	343.15	446.5	586.7	269.6
5.097	983.06	343.16	442.4	584.4	269.5
9.967	985.17	343.14	437.9	581.3	268.7
15.525	987.55	343.15	433.0	577.3	267.5
20.000	989.45	343.15	429.3	573.8	266.0
25.586	991.82	343.14	424.8	568.7	263.5
30.045	993.68	343.16	421.4	564.6	261.2
35.514	995.98	343.15	417.3	558.7	257.7
40.050	997.87	343.15	414.1	553.5	254.4
0.846	974.29	354.24	451.4	655.5	346.1
5.097	976.23	354.25	448.0	654.2	346.7
9.967	978.33	354.27	444.5	652.4	346.8
15.525	980.63	354.27	440.9	649.9	346.1
20.000	982.58	354.27	438.0	647.3	344.9
25.586	984.92	354.27	434.7	643.6	342.8
30.045	986.83	354.28	432.1	640.2	340.5
35.514	989.17	354.27	429.2	635.4	336.8
40.050	991.07	354.27	427.0	631.0	333.3
1.626	962.02	372.90	448.4	730.0	460.6
5.059	963.59	372.90	446.9	732.0	464.0
10.042	965.73	372.96	444.9	734.6	468.5
15.525	968.08	372.97	443.0	736.9	472.2
20.014	970.00	372.99	441.7	738.4	474.6
25.596	972.31	373.00	440.4	739.7	476.5
30.001	974.44	372.90	439.5	740.0	476.7
35.576	976.79	372.91	438.8	740.2	476.8
40.013	978.53	372.92	438.4	740.1	476.2

Table 3. Experimental Values of Pressure, *p*/MPa, Density, ρ/kg·m^{-3}, Temperature, *T*/K, Isothermal Compressibility $k_T \cdot 10^6$/MPa^{-1}, Isobaric Thermal Expansivity, $\alpha_p \cdot 10^6$/K^{-1}, and Difference in Isobaric and Isochoric Heat Capacities, $(c_p - c_v)$/J·kg^{-1}·K^{-1}, of the Sabir-Oba Geothermal Resource of Azerbaijan from $T = (278.01$ to $373.19)$ K

p	P	T	$k_T \cdot 10^6$	$\alpha_p \cdot 10^6$	$c_p - c_v$
1.170	1004.52	278.05	467.7	129.3	9.9
5.040	1006.40	278.04	463.2	133.7	10.7
9.815	1008.57	278.04	458.1	139.1	11.6
15.053	1011.00	278.04	452.5	145.3	12.8
20.012	1013.23	278.04	447.7	151.3	14.0
25.087	1015.52	278.04	442.8	157.7	15.4
30.004	1017.77	278.03	438.3	164.1	16.8
34.977	1019.97	278.02	434.0	170.6	18.3
40.047	1022.20	278.01	429.8	177.5	19.9
1.272	1002.87	288.26	457.5	214.0	28.8
5.052	1004.61	288.22	453.0	216.9	29.8
10.056	1006.88	288.21	447.2	221.3	31.3
15.102	1009.15	288.19	441.6	225.7	33.0
20.031	1011.34	288.17	436.3	230.2	34.6
25.133	1013.58	288.15	431.1	235.1	36.4
30.054	1015.72	288.14	426.3	240.0	38.3
35.116	1017.90	288.13	421.6	245.2	40.4
39.961	1019.96	288.12	417.2	250.3	42.4
0.833	1000.17	298.14	451.2	287.8	54.7
5.150	1002.10	298.16	445.7	290.4	56.3
9.831	1004.17	298.19	439.9	293.4	58.1
15.213	1006.53	298.19	433.6	296.8	60.2
20.054	1008.63	298.19	428.2	300.1	62.2
25.103	1010.80	298.19	422.7	303.6	64.3
30.043	1012.89	298.19	417.5	307.1	66.5
35.133	1015.02	298.19	412.4	311.0	68.9
40.058	1017.07	298.19	407.7	314.8	71.3
1.339	995.32	313.14	445.2	389.9	107.4
5.044	996.96	313.15	440.1	390.5	108.9
9.915	998.97	313.18	433.9	391.6	110.8
15.102	1001.20	313.18	427.3	392.7	112.9
19.876	1003.18	313.18	421.6	393.9	114.9
25.133	1005.49	313.18	415.1	395.4	117.3
29.945	1007.43	313.21	409.8	397.1	119.6
35.102	1009.61	313.19	404.0	398.8	122.1
39.991	1011.64	313.18	398.8	400.6	124.6
1.054	988.76	328.15	446.4	483.8	174.0
4.985	990.47	328.15	440.6	482.8	175.3
10.025	992.64	328.15	433.4	481.6	176.9
15.321	994.89	328.15	426.2	480.6	178.8
20.014	996.86	328.15	420.0	479.9	180.5
25.214	999.02	328.15	413.4	479.3	182.6
30.026	1000.99	328.15	407.5	479.0	184.6
35.057	1003.03	328.15	401.5	478.7	186.7
39.987	1005.01	328.15	395.9	478.6	189.0
1.628	981.01	343.04	453.8	573.2	253.2
5.079	982.59	343.06	447.9	570.8	254.0
9.841	984.56	343.14	440.7	568.3	255.4
15.102	986.93	343.18	432.3	565.2	256.9
20.073	989.01	343.21	425.2	562.6	258.3
25.133	991.16	343.18	418.0	559.8	259.6
30.021	993.22	343.16	411.4	557.4	260.9
35.102	995.19	343.15	405.1	555.2	262.4
40.025	997.20	343.14	398.9	553.2	264.0
1.954	972.22	358.15	466.7	662.6	346.6
5.021	973.61	358.16	461.1	659.1	346.6
10.032	975.87	358.14	452.3	653.5	346.5
15.621	978.32	358.15	442.9	647.8	346.9
20.026	980.22	358.15	435.9	643.6	347.2
25.214	982.40	358.16	427.9	638.9	347.8
29.986	984.39	358.15	420.9	634.8	348.3
35.014	986.44	358.15	413.9	630.7	349.0
39.952	988.42	358.14	407.2	627.0	349.8
1.830	961.98	373.11	487.8	753.7	451.7
5.135	963.33	373.19	481.8	749.3	451.4
10.012	965.52	373.19	472.4	741.8	450.2
15.104	967.96	373.15	462.2	733.6	448.8
20.001	970.19	373.11	453.3	726.3	447.6
25.166	972.40	373.15	444.5	719.7	447.2
29.948	974.38	373.16	436.8	713.9	446.8
35.205	976.60	373.16	428.5	707.5	446.4
39.915	978.56	373.16	421.3	702.1	446.2

WIKA Alexander Wiegand GmbH & Co., Germany) with a measuring error of 0.1 %. All high pressure valves (2, 7, 8, 16, 17), tubes, fittings (3 and 11), and so on were supplied by SITEC and NOVA (Switzerland).

The mPDS 2000V3 evaluation unit displays the oscillating period with seven digits, which, according to the specification of Anton-Paar, corresponds to an uncertainty on the order of 0.01 kg m^{-3} related only to the measured oscillating period; however, as a result of uncertainties of the temperature, the pressure, and the period of oscillation measurements for reference samples, vacuum, and measured liquid, the overall experimental uncertainty in the reported density values at temperatures $T = (298.15$ to $398.15)$ K and at pressures up to $p = 40$ MPa is within $\Delta\rho = \pm(0.1$ to $0.3)$ kg·m^{-3}.

Rearrangement of the equation and substitution of the mechanical constants lead to the classical equation for vibrating tube densimeters

$$\rho(T,p) = A(T,p) - B(T,p)\tau^2(T,p) \tag{2}$$

where $\rho(T, p)$ is the sample density in kilograms per cubic meter and $\tau(T, p)$ is the period of oscillation in microseconds. The parameters $A(T, p)$ and $B(T, p)$ were determined by substance calibration measuring the period of oscillation of at least two samples with known density. Water (distillate) and NaCl(aq) in various molalities were used as reference substances for the calibration of the installation.[9−11] The measurements of the period of vacuum as a function of the temperature have been performed after having created a minimal pressure ((3 to 5) Pa).

Unfortunately, the parameters $A(T, p)$ and $B(T, p)$ are highly temperature- and pressure-dependent. Therefore, the parameters must be determined for each temperature and pressure separately or, like in this work, the classical equation must be expanded with temperature and pressure-dependent terms. For measurements at $T = (298.15$ to $398.15)$ K and up to $p = 40$ MPa, an extended calibration equation with 14 significant parameters is employed[12]

$$A(T,p) = \sum_i a_i (T/\mathrm{K})^i + \sum_j b_j (p/\mathrm{MPa})^j + c(T/\mathrm{K})(p/\mathrm{MPa}) \tag{3}$$

$$B(T,p) = \sum_i d_i (T/\mathrm{K})^i + \sum_j e_j (p/\mathrm{MPa})^j + f(T/\mathrm{K})(p/\mathrm{MPa}) \tag{4}$$

where a_0, a_1, a_2, a_3, b_1, b_2, c, d_0, d_1, d_2, d_3, e_1, e_2, and f are the parameters of the these extended vibrating tube equations.

Before experiments, the installation was washed with water and acetone and was dried using the vacuum system. The valve of the flask (1) closed. Vacuum is applied over (3 to 4) h using a vacuum pump (19) (model S 1.5, Leybold, Germany) until a minimal pressure ((3 to 5) Pa) has been reached (measured with digital vacuum indicator (10) Thermovac TM 100 (Leybold, Germany)). The valve (17) is closed, and the valve of the flask (1) is opened. The investigated substance is fills the measuring system. For the tracing of flow of the measured sample, a special window (12) was constructed between valves (16) and (17). After filling of the system, valves (2) and (16) were closed. The high-pressure region is located between these two valves (bold lines in Figure 2). The experiments were usually started at low pressure in the measured cell ((0.8 to 1.0) MPa). For temperature stabilization, the waiting time is about (50 to 60) min. The period of oscillation of the vibration tube is taken from the display of the mPDS2000V3 control system (9).

Samples were collected directly from the resources. The Khachmaz geothermal resource is at $T = 329.75$ K and the Sabir-Oba geothermal resource is at $T = 348.15$ K. The geographical coordinates of the resources are 41°27′18″N and 48°47′21″E (Khachmaz) and 41°30′82″N and 48°45′32″E (Sabir-Oba).

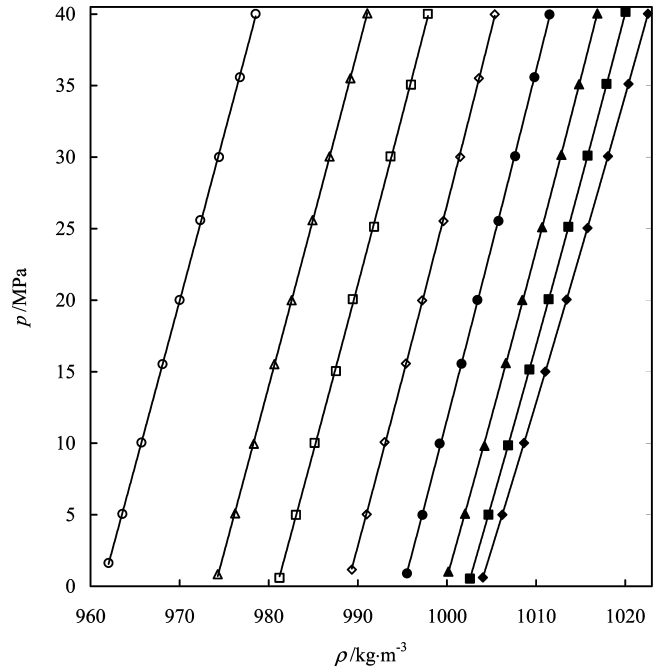

Figure 3. Plot of pressure, p, of Khachmaz geothermal water versus density, ρ: ◆, 278.15 K; ■, 288.16 K; ▲, 298.17 K; ●, 313.18 K; ◇, 328.18 K; □, 343.15 K; △, 354.27 K; ○, 372.96 K; —, calculated by eqs 5 and 6.

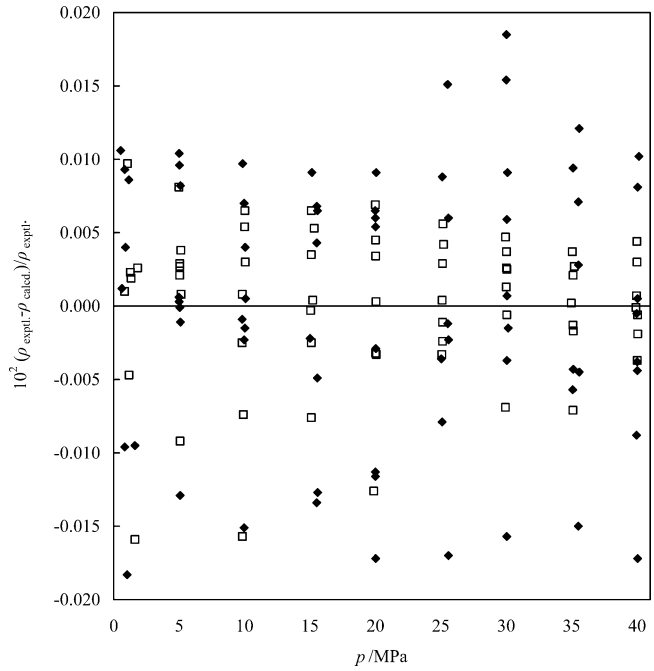

Figure 5. Plot of deviations of experimental density, ρ_{exptl}, of the investigated geothermal resources of Azerbaijan from the density calculated by eqs 5 and 6, ρ_{calcd}, versus pressure, p: ◆, Khachmaz; □, Sabir-Oba.

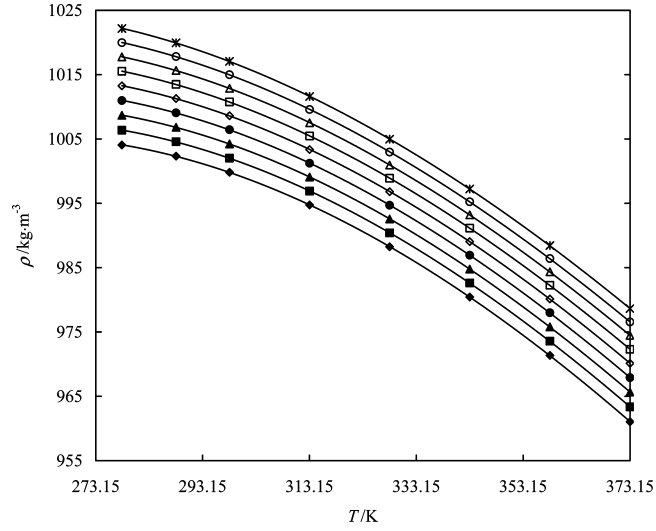

Figure 4. Plot of density, ρ, of Sabir-Oba geothermal water versus temperature, T: ◆, 0.101 MPa; ■, 5 MPa; ▲, 10 MPa; ●, 15 MPa; ◇, 20 MPa; □, 25 MPa; △, 30 MPa; ○, 35 MPa; *, 40 MPa.

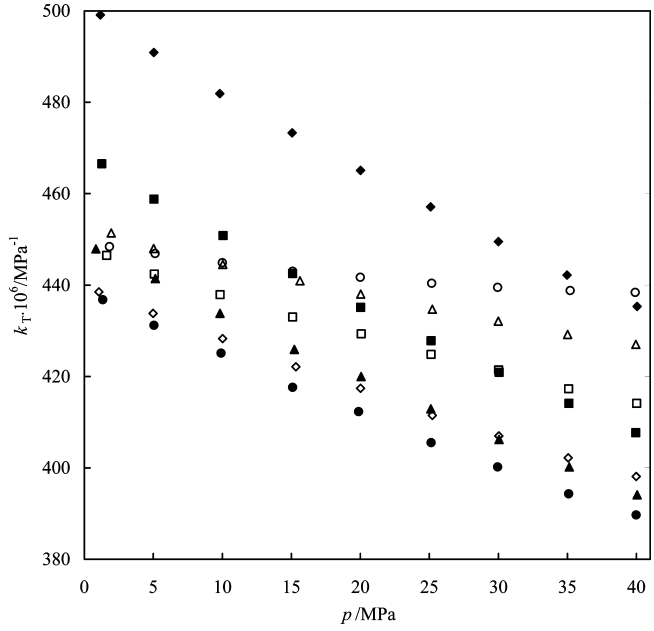

Figure 6. Plot of isothermal compressibility, $k_T \cdot 10^6/\mathrm{MPa}^{-1}$, of Khachmaz geothermal water versus pressure, p: ◆, 278.15 K; ■, 288.15 K; ▲, 298.15 K; ●, 313.15 K; ◇, 328.18 K; □, 343.15 K; △, 354.27 K; ○, 372.96 K.

The samples were filtered and degassed slowly using the vacuum system (10, 19, 20). To stop vaporization of pure water, the vacuum procedure was very slow. (The groove of the flask valve, which held the sample, was very slightly opened.) We tried to use the samples as close as possible to their original state (T, p) but at the same time to remove all dissolved gases and nonmineral compounds. The amount of dissolved gases or

Table 4. Values of the Coefficients a_i, b_i, and c_i in Equations *5* and *6*

a_i	b_i	c_i
	Geothermal Water "Khachmaz"	
$a_1 = -3.9508587$	$b_0 = 8322.6444921$	$c_0 = -6583.286607275$
$a_2 = 0.019210690563$	$b_1 = -56.828468335$	$c_1 = 45.23492762848$
$a_3 = -0.\ 3685081337 \cdot 10^{-4}$	$b_2 = 0.103286734291$	$c_2 = -0.07893862924$
	Geothermal Water "Sabir-Oba"	
$a_1 = -5.2005650454$	$b_0 = 2109.877821027$	$c_0 = -1182.2695455815$
$a_2 = 0.01502325482$	$b_1 = -7.479806751$	$c_1 = 4.8600740508$
$a_3 = -0.108475601 \cdot 10^{-4}$	$b_2 = 0.927626176 \cdot 10^{-2}$	$c_2 = -0.52655191 \cdot 10^{-2}$

Table 5. Statistical, Absolute, and Average Deviations of Equations *5* and *6*

standard deviation[a]	absolute deviation[b]	maximum absolute deviation	average percent deviation[c]
kg·m^{-3}	kg·m^{-3}	kg·m^{-3}	%
Geothermal Water "Khachmaz"			
0.09	0.07	0.184	0.007
Geothermal Water "Sabir-Oba"			
0.05	0.04	0.156	0.004

[a] Standard deviation: STD = $[(\sum(\rho_{exptl} - \rho_{calcd})^2)/(n - 1)]^{1/2}$. [b] Absolute deviation: ABD = $(1/n)\ \sum|\rho_{calcd} - \rho_{exptl}|$. [c] Average percent deviation: AAD = $(100/n)\ \sum|(\rho_{exptl} - \rho_{calcd})/\rho_{exptl}|$, where ρ_{exptl} is the experimental density, ρ_{calcd} is the density obtained by fitting of eqs 5 and 6, and n is the number of experimental points.

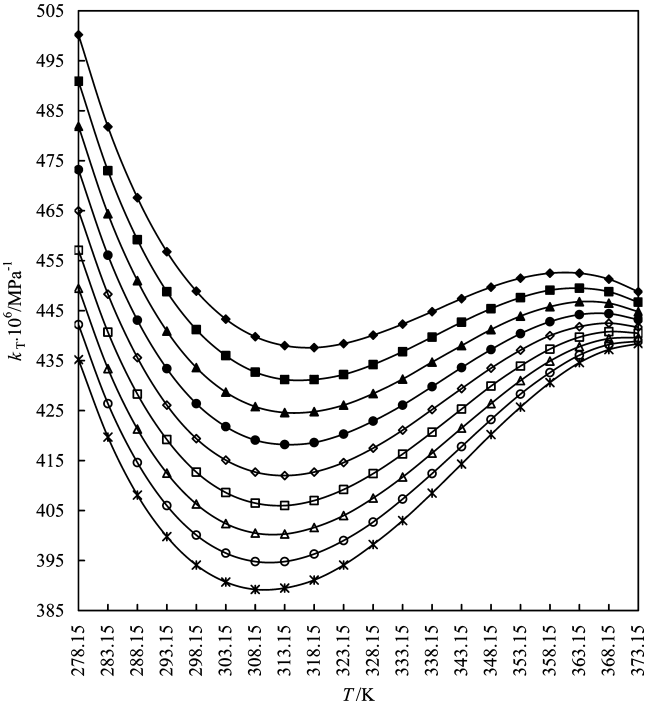

Figure 7. Plot of isothermal compressibility, $k_T \cdot 10^6$/MPa^{-1}, of Khachmaz geothermal water versus temperature, T: ◆, 0.101 MPa; ■, 5 MPa; ▲, 10 MPa; ●, 15 MPa; ◇, 20 MPa; □, 25 MPa; △, 30 MPa; ○, 35 MPa; *, 40 MPa; solid lines show only character of property changing.

air plays a very negative role in the density measurements, especially at high temperatures.

Results and Discussion

The chemical compounds of the Khachmaz and Sabir-Oba geothermal resources were analyzed in the IRIS Intrepid II OES, and the results of analysis are shown in Table 1.

The (p, ρ, T) properties of the Khachmaz and Sabir-Oba geothermal resources of the Khachmaz region of Azerbaijan at T = (278.15 to 373.15) K and at pressures up to p = 40 MPa are reported. The obtained (p, ρ, T) results are listed in Tables 2 and 3, respectively.

Using a program for standard thermodynamic analysis to describe the (p, ρ, T) properties of the geothermal waters, we used the equation of state from ref 13

$$p = A(T)\rho^2 + B(T)\rho^8 + C(T)\rho^{12} \qquad (5)$$

where the coefficients of eq 5 $A(T)$, $B(T)$, and $C(T)$ are functions of temperature.

$$A(T) = \sum_{i=1}^{3} a_i T^i, \quad B(T) = \sum_{i=0}^{2} b_i T^i, \quad C(T) = \sum_{i=0}^{2} c_i T^i \qquad (6)$$

a_i, b_i, and c_i are the coefficients of the polynomials given in Table 4 together with the standard deviation of the fitting in Table 5. Equations 5 and 6 describe the experimental results of the investigated Khachmaz and Sabir-Oba geothermal resources with $\Delta\rho = \pm 0.007$ % and $\Delta\rho = \pm 0.004$ % average percent deviations, respectively.

Figures 3, 4, and 5 show plots of pressure, p, of Khachmaz geothermal water versus density, ρ; of density, ρ, of the "Sabir-Oba" geothermal water versus temperature, T, at round pressures calculated by eqs 5 and 6; and deviations of experimental density, ρ_{exptl}, of geothermal resources from the calculated density, ρ_{calcd}, by eqs 5 and 6 versus pressure, p.

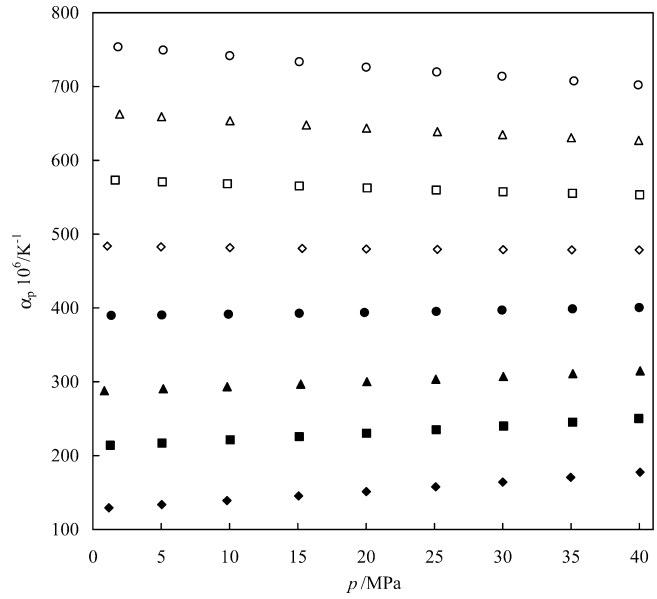

Figure 8. Plots of isobaric thermal expansibility, $\alpha \cdot 10^6$/K^{-1}, of Sabir-Oba geothermal water versus pressure, p: ◆, 278.05 K; ■, 288.15 K; ▲, 298.19 K; ●, 313.18 K; ◇, 328.15 K; □, 343.18 K; △, 358.15 K; ○, 373.15 K.

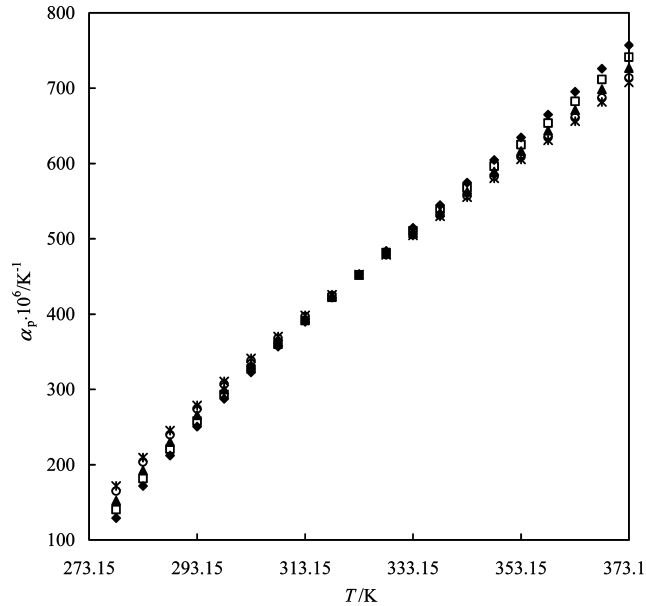

Figure 9. Plot of isobaric thermal expansibility, $\alpha_p \cdot 10^6$/K^{-1}, of Sabir-Oba geothermal water versus temperature, T: ◆, 0.101 MPa; □, 10 MPa; ▲, 20 MPa; ○, 30 MPa; *, 40 MPa.

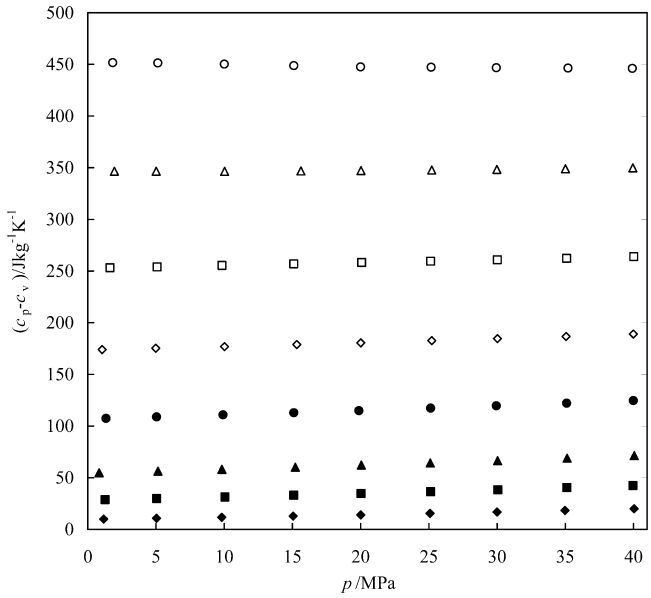

Figure 10. Plot of difference in isobaric and isochoric heat capacities, $(c_p - c_v)$/J·kg^{-1}·K^{-1}, of Sabir-Oba geothermal water versus pressure, p: ◆, 278.05 K; ■, 288.15 K; ▲, 298.19 K; ●, 313.18 K; ◇, 328.15 K; □, 343.18 K; △, 358.15 K; ○, 373.15 K.

The isothermal compressibility, k_T/MPa^{-1}, is a measure of the relative volume change of a fluid as a response to a pressure change at constant temperature

$$k_T = (1/\rho)(\partial p/\partial \rho)_T^{-1} \tag{7}$$

It can be calculated from the experimental (p, ρ, T) results of geothermal sources by using eqs 5 and 6 as follows

$$k_T = 1/(2A\rho^2 + 8B\rho^8 + 12C\rho^{12}) \tag{8}$$

The calculated values of the isothermal compressibility are given in Tables 2 and 3 and are shown in Figure 6 versus temperature and Figure 7 versus pressure.

The other thermal coefficient that can be calculated from eqs 5 and 6 is the isobaric thermal expansibility, α_p/K^{-1}, which is the tendency of matter to change in volume in response to a change in temperature at constant pressure. When a sample is heated, its constituent particles move around more vigorously and by doing so generally maintain a greater average separation. Samples that contract with an increase in temperature are very uncommon; this effect is limited in size and occurs only within limited temperature ranges. The degree of expansion divided by the change in temperature is called the sample's coefficient of thermal expansibility and generally varies with temperature.

$$\alpha_p = (1/\rho)(\partial p/\partial T)_\rho (\partial p/\partial \rho)_T^{-1} \tag{9}$$

It can also be calculated from the experimental (p, ρ, T) results of the geothermal resources by using eqs 5 and 6

$$\alpha_p = [A'(T) + B'(T)\rho^6 + C'(T)\rho^{10}]/[2A(T) + 8B(T)\rho^6 + 12C(T)\rho^{10}] \tag{10}$$

where $A'(T)$, $B'(T)$, and $C'(T)$ are the derivatives of $A(T)$, $B(T)$, and $C(T)$ in the following form

$$A'(T) = \sum_{i=1}^{3} i a_i T^{i-1},$$

$$B'(T) = \sum_{i=1}^{2} i b_i T^{i-1},$$

$$C'(T) = \sum_{i=1}^{2} i c_i T^{i-1} \tag{11}$$

The calculated values of the isobaric thermal expansibilities are given in Tables 2 and 3 and are shown for Sabir-Oba geothermal water in Figure 8 versus pressure and Figure 9 versus temperature.

The next important parameter for the investigation is the difference in specific heat capacities $(c_p - c_v)$/J·kg^{-1}·K^{-1}. Measuring the heat capacity at constant volume can be prohibitively difficult for liquids. That is, small temperature changes typically require large pressures to maintain a liquid at constant volume, which implies that the containing vessel must be nearly rigid or at least very strong. Instead, it is easier to measure the heat capacity at constant pressure and to solve for the heat capacity at constant pressure using mathematical relationships derived from the basic thermodynamic laws

$$c_p = c_v + T\frac{(\partial p/\partial T)_\rho^2}{\rho^2(\partial p/\partial \rho)_T} \tag{12}$$

where c_p and c_v are the heat capacities at constant pressure and volume, respectively. Using eqs 7 and 9, we can find the following relationship

$$c_p - c_v = \frac{\alpha_p^2 T}{\rho k_T} \tag{13}$$

The calculated values of the differences in specific heat capacities are given in Tables 2 and 3 and are shown in Figure 10.

Conclusions

New density measurements of two geothermal resources of Azerbaijan at T = (278.15 to 373.15) K and pressures up to p = 40 MPa are reported using a vibration tube densimeter. The chemical analysis was carried out using a modern IRIS Intrepid II OES. The densities of the samples at high temperatures and pressures were investigated for the first time. A selected equation of state was used to calculate the various volumetric properties such as isothermal compressibility, isobaric thermal expansibility, and difference in isobaric and isochoric heat capacities.

The isothermal compressibility values of the geothermal resources of Azerbaijan have same anomalies, such as pure water. The main part of these samples (approximately 99.9 %) is water. In a typical liquid, the compressibility decreases as the structure becomes more compact because of lowered temperature. In water and all aqueous solutions of salts, where the concentration of water is high, the cluster equilibrium shifts toward the more open structure (for example, expanded structure (ES)) as the temperature is reduced because it favors the more ordered structure. (That is, ΔG for ES ⇌ CS (collapsed structure) becomes more positive.) Because the water structure is more open at these lower temperatures, the capacity for it to be compressed increases.[14] The effect is not a simple dependency on density, however, or else the minimum would be at T = 319.65 K for isothermal (that is, without change in temperature) compressibility of pure water. The compressibility depends on fluctuations in the specific volume, and these will

be large where water molecules fluctuate between being associated with a more open structure or not and between the different environments within the water clusters. At high pressures (for example, ~200 MPa) this compressibility anomaly, although still present, is far less apparent.[15] The temperature- and pressure-dependent anomalies of isothermal compressibility are presented in Figures 6 and 7.

The isobaric thermal expansibility of geothermal resources increases with increased pressure up to about $T = 313.18$ K (in which the isobaric thermal expansibility is approximately constant), which is in contrast with most other liquids where thermal expansion decreases with increased pressure. After $T = 313.18$ K, isobaric thermal expansibility of geothermal resources decreases with increased pressure. This is due to the collapsed structure of water having a greater thermal expansibility than the expanded structure and the increasing pressure shifting the equilibrium toward a more collapsed structure. The temperature- and pressure-dependent anomalies of isobaric thermal expansibility are presented in Figures 8 and 9.

Acknowledgment

We thank Frau Silvia Berndt (University of Rostock) for her assistance in the chemical analysis of the samples.

Literature Cited

(1) Ismailova, M. M. Environmental problems associated with utilization of mineral waters in urbanized areas of Azerbaijan. *NATO Sci. Ser.* **2006**, *74*, 279–288.
(2) Ibrahimova, I. Sh.; Tagiyev, I. I.; Babayev, A. A. *Resources of Mineral & Thermal Waters of Azerbaijan*; Chashiogly, Azerbaijan, 2001.
(3) Ibrahimova, I. Sh. *Application of GIS to Available Information on Thermal Waters in the Azerbaijan Republic and Its Usefulness for Environmental Assessment*; The United Nations University Geothermal Training Programme Report Number 10: Reykjavík, Iceland, 2006.
(4) Gashgay, M. A. *Mineral Sources of Azerbaijan, Baku*, 1952.
(5) Askerov, A. G. *Mineral Sources of Azerbaijan SSR, Baku*, 1954.
(6) Ramazanov, K. Azerbaijan's geothermal energy potential. *IGA News* **1994**, *16*, 5.
(7) Babayev, A. A.; Ibrahimova, I. Sh. Structural-tectonic features of accommodation deposits of mineral waters of Azerbaijan and their complex development. *Environ. Geol.* **2004**, *5*, 20–23.
(8) Kratky, O.; Leopold, H.; Stabinger, H. H. Dichtemessungen an Flüssigkeiten und Gasen auf 10^{-6} g/cm^3 bei 0.6 cm^3 Präparatvolumen. *Z. Angew. Phys.* **1969**, *27*, 273–277.
(9) Wagner, W.; Pruss, A. The IAPWS formulation 1995 for the thermodynamic properties of ordinary water substance for general and scientific use. *J. Phys. Chem. Ref. Data* **2002**, *31*, 387–535.
(10) Hilbert, R. *pVT-Daten von Wasser und von wässrigen Natriumchlorid-Lösungen bis 873 K, 4000 Bar und 25 Gewichtsprozent NaCl*; Hochschul Verlag: Freiburg, Germany, 1979; p 209.
(11) Archer, D. G. Thermodynamic properties of the NaCl + H_2O system. II. Thermodynamic properites of NaCl(aq), NaCl·$2H_2O$(cr) and phase equilibria. *J. Phys. Chem. Ref. Data* **1992**, *21*, 793–829.
(12) Ihmels, E. C.; Gmehling, J. Densities of toluene, carbon dioxide, carbonyl sulfide, and hydrogen sulfide over a wide temperature and pressure range in the sub- and supercritical state. *Ind. Eng. Chem. Res.* **2001**, *40*, 4470–4477.
(13) Safarov, J. T. The investigation of the (p, ρ, T) and (p_s, ρ_s, T_s) properties of {(1− x)CH_3OH + xLiBr} for the application in absorption refrigeration machines and heat pumps. *J. Chem. Thermodyn.* **2003**, *35*, 1929–1937.
(14) Kell, G. S. Density, thermal expansivity, and compressibility of liquid water from 0° to 150 °C: correlations and tables for atmospheric pressure and saturation reviewed and expressed on 1968 temperature scale. *J. Chem. Eng. Data* **1975**, *20*, 97–105.
(15) Kanno, H.; Angell, C. A. Water: anomalous compressibilities to 1.9 kbar and correlation with supercooling limits. *J. Chem. Phys.* **1979**, *70*, 4008–4016.

Received for review November 9, 2008. Accepted March 14, 2009.

JE800840M